

## High-resolution spectroscopy of the old, high-latitude open cluster UBC 1052

Donada, J.<sup>1,2,3</sup>, Casamiquela, L.<sup>4</sup>, Anders, F.<sup>1,2,3</sup>, Luri, X.<sup>1,2,3</sup>, Balaguer-Núñez, L.<sup>1,2,3</sup>, Blanco-Cuaresma, S.<sup>5,6</sup>, Slumstrup, D.<sup>7</sup>, Castro-Ginard, A.<sup>1,2,3</sup>, Jordi, C.<sup>3</sup>, Carbajo-Hijarrubia, J.<sup>1,2,3</sup>, Carrera, R.<sup>8</sup> and Carrasco, J. M.<sup>1,2,3</sup>

<sup>1</sup> Institut de Ciències del Cosmos (ICCUB), Universitat de Barcelona (UB), Martí i Franquès 1, E-08028 Barcelona, Spain

<sup>2</sup> Departament de Física Quàntica i Astrofísica (FQA), Universitat de Barcelona (UB), Martí i Franquès 1, E-08028 Barcelona, Spain

<sup>3</sup> Institut d'Estudis Espacials de Catalunya (IEEC), Esteve Terradas, 1, Edifici RDIT, Campus PMT-UPC, 08860 Castelldefels (Barcelona), Spain

<sup>4</sup> GEPI, Observatoire de Paris, PSL Research University, CNRS, Sorbonne Paris Cité, 5 place Jules Janssen, 92190, Meudon, France

<sup>5</sup> Harvard-Smithsonian Center for Astrophysics, 60 Garden Street, Cambridge, MA 02138, USA

<sup>6</sup> Laboratoire de Recherche en Neuroimagerie, University Hospital (CHUV) and University of Lausanne (UNIL), Lausanne, Switzerland

<sup>7</sup> European Southern Observatory, Alonso de Córdova 3107, Vitacura, Santiago, Chile

<sup>8</sup> INAF-Osservatorio di Astrofisica e Scienza dello Spazio di Bologna, via P. Gobetti 93/3, 40129, Bologna, Italy

### Abstract

The publication of the *Gaia* data releases has recently led to a drastic improvement in both the census of Galactic open clusters (OCs) and their characterisation, but still only a small fraction of them has been studied spectroscopically at high resolution to date. In this study we perform a detailed spectroscopic analysis of UBC 1052, an old OC located at a galactocentric radius  $R_{GC} \sim 6$  kpc which has the peculiarity of being at a considerably high latitude ( $z \sim 350$  pc). We use high-resolution spectra acquired with UVES-FLAMES at the VLT to derive high-precision abundances of a wide variety of chemical species. Its inferred metallicity, slightly supersolar ( $[Fe/H] = 0.05 \pm 0.02$  dex), is significantly smaller than the typical metallicities displayed by OCs at similar  $R_{GC}$ , thus placing UBC 1052 as a candidate for an inner-migrator open cluster.

## 1 Introduction

Open clusters (OCs) are excellent tracers of the overall history of star formation and nucleosynthesis across the Galactic disc’s lifetime. The ESA *Gaia* space mission data releases (DRs, DR3 being the latest: [10]) have led to a drastic improvement in both the census of OCs and their characterisation (see [5] for a recent review). Using EDR3, [9] identified several hundred of new OCs. Among them, some particularly exciting OCs were found at high Galactic latitudes. They are old, and located at heights beyond the typical thin disc scaleheight (both above and below the Galactic mid-plane). Since most star formation takes place in the thin disc, it is of great interest to perform spectroscopic follow-up observations of these OCs far from the Galactic mid-plane to explore their nature and what their chemical abundances can reveal about their origin. It was in this context that we obtained spectroscopic data for one such cluster, UBC 1052, which is an old OC located at a galactocentric radius  $R_{GC} \sim 6$  kpc and at  $\sim 350$  pc above the Galactic mid-plane.

## 2 Data

UBC 1052 was discovered in [9], who used *Gaia* EDR3 data down to  $G = 18$  mag and applied DBSCAN clustering algorithm, identifying 31 members. Later, it was also detected by [14], who used *Gaia* DR3 data down to  $G = 20$  mag and applied HDBSCAN clustering algorithm, identifying 59 members (28 in common with [9]). This membership list likely includes more contaminants than [9] (see central panel of Fig. 1 and large parallax dispersion in Table 1).

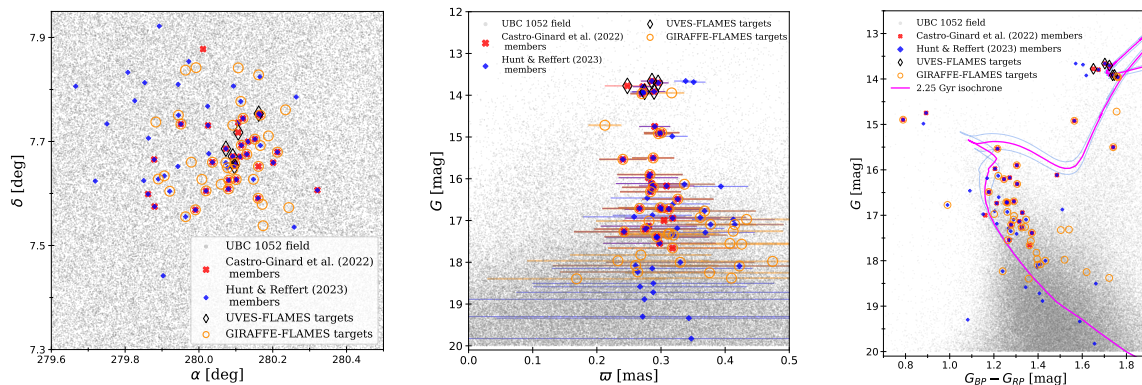


Figure 1: On-sky projection of UBC 1052 (*left*), *Gaia* DR3  $G$ -band magnitude as a function of the parallax (*centre*), and *Gaia* observed colour-magnitude diagram and fitted isochrones from [17] (*right*) for the cluster field (grey dots), for UBC 1052 members in [9] (red crosses) and in [14] (blue squares), and for the targets we observed using UVES-FLAMES (black diamonds) and GIRAFFE-FLAMES (orange circles).

The target selection was based on the [9] catalogue and *Gaia* DR3 observables, since [14] had not been released yet. We acquired spectra of 46 potential cluster members (shown in Fig. 1) using FLAMES, the multi-object spectrograph of the VLT (ESO) which feeds

two different instruments covering the entire visual spectral range: GIRAFFE and UVES. With UVES we acquired high-resolution ( $R \sim 47\,000$ ), high-S/N (70-80) spectra of five red clump (RC) stars, and used them to derive high-precision chemical abundances of the cluster (Section 4.2). GIRAFFE fibres were used to acquire medium-resolution spectra of 41 targets distributed across the cluster’s CMD using 3 different gratings: HR11: [559, 584] nm ( $R \sim 27\,000$ ), HR13: [611, 640] nm ( $R \sim 24\,000$ ), HR14A: [630, 669] nm ( $R \sim 17\,000$ ). The primary purpose of these spectra is to assess their cluster membership (ongoing work).

Due to the limitations posed by the fibre positioners, we could not observe several of the members in [9]. In the end, out of the 46 observed stars, 31 are members of UBC 1052 (21 belong to [9] and 29 belong to [14]), and 15 do not belong to any of the two membership lists.

### 3 Spectroscopic analysis

We perform a 1D LTE spectroscopic analysis using the spectral synthesis technique implemented in the public code *iSpec* ([4], [3]), the radiative transfer code SPECTRUM ([11]), MARCS atmospheric models ([12]), and the data of atomic absorption lines from version 6 of the *Gaia*-ESO line list ([13]). This line list includes hyperfine structure and isotope splitting data, and its line recommendations are taken into consideration.

For the red clump stars observed with UVES, we obtain their atmospheric parameters (effective temperature,  $T_{\text{eff}}$ , and surface gravity,  $\log g$ ), radial velocities, and chemical abundances for a wide variety of species.

For the vast majority of elements (filled symbols in Fig. 2), a strictly line-by-line differential analysis is performed (as done in e.g. [15]): to the absolute abundance of each selected line, we subtract the absolute abundance of that line from a RC star in M67 OC (*Gaia* DR3 604918144751101440, using its publicly available UVES spectra). Our estimated  $T_{\text{eff}}$  and  $\log g$  for this reference star in M67 are compatible with the atmospheric parameters of the studied UBC 1052 RC stars. We compute the mean of this difference over the lines of each element and later over the four selected RC stars (see Section 4.1 for the selection) to get the mean abundances in UBC 1052 with respect to the RC star in M67. These values are subsequently translated to the solar scale by performing an equivalent strictly line-by-line differential analysis of a solar analogue in M67 OC (M67-1194, [18], we use its publicly available UVES spectra) with respect to the Sun (using the spectrum ‘UVES.Sun-1’ of the *Gaia* FGK Benchmark Stars library). We assume that the abundances of the RC star in M67 and of the solar analogue in M67 are compatible within the uncertainties for the studied elements (whose abundances are not affected by stellar evolution as opposed to e.g. Na, [16]).

For the three elements for which a differential analysis is not possible (open symbols in Fig. 2), we directly compute their mean absolute abundance (over all the selected lines for one star and then over the four UBC 1052 RC stars) and subtract to it the solar photospheric abundance of this element from [2]. In the case of Eu and Zr, the differential analysis is not possible because their abundances cannot be confidently derived for the solar analogue in M67.

## 4 Results

### 4.1 Cluster parameters

Table 1 shows UBC 1052’s parameters inferred by [9], [14], and in the present work. [9] and [14] used different neural networks to estimate the distance, line-of-sight interstellar extinction  $A_V$ , and age in an industrial fashion for all the OCs in their large samples. Such automatic methods for the estimation of the cluster’s parameters are known to perform poorly in some instances (e.g. for OCs which are not highly populated or which lack a clearly defined main sequence and turn-off). To estimate the distance, we used the members in [9] and performed a Bayesian distance estimation for the zero-point corrected parallax of these members assuming negligible parallax correlations and cluster extent. To compute a rough estimate of the extinction, we check out the parameters from *StarHorse2021* ([1]) for the cluster region (computed assuming the sources are field stars), and obtain a mean extinction for the members in [9] of  $A_V = 1.23 \pm 0.03$  mag. To estimate the age we represent the cluster’s CMD using the members in [9] and [14] (right panel of Fig. 1), and visually fit to it PARSEC v2.0 isochrones ([17]) with metallicity  $[M/H] = +0.05$  dex (see Section 4.2) and rotation rate  $\omega_i = 0.3$ . We obtain an age of  $2.25 \pm 0.25$  Gyr (isochrones in the right panel of Fig. 1: pink for the nominal value, light purple for the uncertainty limits). The younger ages retrieved with neural networks may be caused by the presence of blue straggler stars which disrupt the isochrone fits ([14]). Using the UVES spectra of our sample of five RC stars, we find a clear outlier in radial velocity ( $V_{\text{rad}}$ ), which is precisely the only UVES target which does not belong to both catalogues. Furthermore, its chemical analysis reveals that it also has discrepant abundances. We therefore consider this star a potential non-member and exclude it from the analysis. Our computed mean  $V_{\text{rad}}$  of the remaining four RC stars of the cluster is compatible with the mean *Gaia*  $V_{\text{rad}}$  for the members in both catalogues (Table 1).

Table 1: UBC 1052 parameters from [9] (31 members), from [14] (59 members), and from the present study (using the members in [9] for the distance and  $A_V$ , in [9] and [14] for the age, and UVES spectra for four red clump stars for  $V_{\text{rad}}$ , see text).

	Castro-Ginard et al. 2022 ([9])	Hunt & Reffert 2023 ([14])	This study
$\overline{\varpi} \pm \sigma_{\varpi}$ (mas)	$0.29 \pm 0.02$	$0.31 \pm 0.04$	
Distance (kpc)	3.840 [3.552, 4.128]	2.994 [2.954, 3.036]	$3.12 \pm 0.07$
$A_V$ (mag)	1.30 [1.15, 1.45]	1.65 [1.43, 1.87]	$1.23 \pm 0.03$
Age (Gyr)	1.58 [1.12, 2.24]	0.92 [0.66, 1.44]	$2.25 \pm 0.25$
$\overline{V}_{\text{rad}}$ (km/s)	$36.7 \pm 3.3$	$35.2 \pm 1.9$	$34.0 \pm 0.5$

### 4.2 Chemical abundances

The mean  $T_{\text{eff}}$  and  $\log g$  we have derived for the four RC members of UBC 1052 are  $4701 \pm 18$  K and  $2.49 \pm 0.02$  dex, respectively. The means of their solar-scaled abundances of 22

chemical species are shown in Fig. 2. For Eu, Zr and Na, they have not been computed differentially and thus the uncertainties are larger on average. For all the other elements, they have been derived through a strictly line-by-line differential analysis, achieving typical precisions of  $\sim 0.025$  dex. For comparison, we also show the results for four OCs which have also been studied through a strictly line-by-line differential analysis ([8] and [7]): two intermediate-age OCs in the solar neighbourhood (Hyades and Praesepe), and two OCs slightly older than UBC 1052 which are also roughly at  $R_{GC} \sim 8$  kpc (Ruprecht 147, in the solar neighbourhood, and UBC 274, located at 1780 pc from the Sun in the fourth Galactic quadrant). We find that UBC 1052 (at  $R_{GC} \sim 6$  kpc) is slightly supersolar ( $[Fe/H] = 0.05 \pm 0.02$  dex), its metallicity being compatible with that of Ruprecht 147, which is located roughly 2 kpc further out in galactocentric radius. UBC 1052 has a chemical signature compatible with that of the other four OCs, with the exceptions of Si ( $\alpha$ -element), Mn (Fe-peak element) and the  $s$ -process elements Y and Nd.

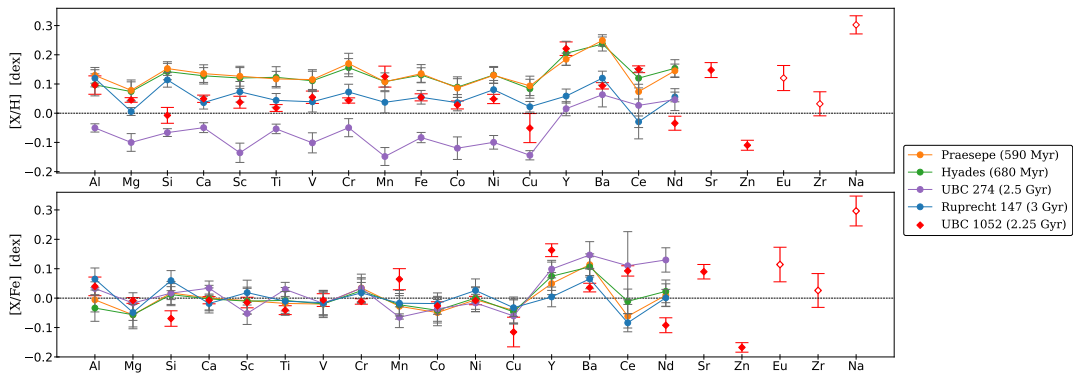


Figure 2: Solar-scaled chemical abundances of the studied open cluster UBC 1052 (in red, differential analysis for the filled symbols and non-differential for the open ones), and of two younger and two older open clusters (computed through the same procedure, [8] and [7]).

## 5 Discussion

Figure 3 shows the radial metallicity gradient in the Milky Way traced by OCs. There is a considerable abundance scatter at a certain  $R_{GC}$ , which is generally attributed to the fact that OCs have undergone radial migration throughout their lifetimes caused by non-axisymmetric structures such as the spiral arms (in addition to possible effects caused by the azimuthal dependence of the abundances). Despite this scatter and the fact that the inner part of the Galaxy is poorly sampled, UBC 1052's metallicity appears to be significantly smaller than the typical metallicities of OCs at  $R_{GC} \sim 6$  kpc (its uncertainty being remarkably smaller than those of the other inner disc OCs). Considering the radial metallicity gradient fit in [19], UBC 1052 is also found to be underabundant, falling outside the 68% confidence interval at its  $R_{GC}$ . This suggests that UBC 1052 is an inner radial migrator: it formed in an outer part of the disc and has migrated to its current position. We aim to analyse its orbit to investigate the inner migration scenario and assess whether its high latitude is related to

some orbital peculiarity which has allowed this OC to survive for over 2 Gyr without having been disrupted.

Finally, some abundance ratios show steep trends with age for OCs (known as chemical clocks). In the case of the age dependencies of  $[Y/Mg]$  and  $[Y/Al]$ , for example, UBC 1052's location is compatible with the expected trend and within the typical scatter at its age.

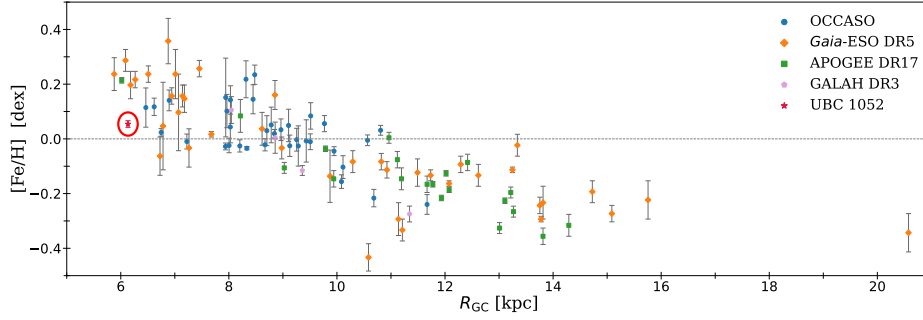


Figure 3: Radial metallicity gradient traced by the open cluster sample gathered in [6] (collection of four high-resolution spectroscopic surveys), adding UBC 1052 (circled red star).

## References

- [1] Anders, F., Khalatyan, A., Queiroz, A. B. A., et al. 2022, *A&A*, 658, A91
- [2] Asplund, M., Amarsi, A. M., & Grevesse, N. 2021, *A&A*, 653, A141
- [3] Blanco-Cuaresma, S. 2019, *MNRAS*, 486, 2075
- [4] Blanco-Cuaresma, S., Soubiran, C., Heiter, U., & Jofré, P. 2014, *A&A*, 569, A111
- [5] Cantat-Gaudin, T., & Casamiquela, L. 2024, *New Astronomy Reviews*, 99, 101696
- [6] Carbajo-Hijarrubia, J., Casamiquela, L., Carrera, R., et al. 2024, *A&A*, 687, A239
- [7] Casamiquela, L., Olivares, J., Tarricq, Y., et al. 2022, *A&A*, 664, A31
- [8] Casamiquela, L., Tarricq, Y., Soubiran, C., et al. 2020, *A&A*, 635, A8
- [9] Castro-Ginard, A., Jordi, C., Luri, X., et al. 2022, *A&A*, 661, A118
- [10] Gaia Collaboration (Vallenari, A., et al.) 2023, *A&A*, 674, A1
- [11] Gray, R., & Corbally, C. 1994, *AJ*, 107, 742
- [12] Gustafsson, B., Edvardsson, B., Eriksson, K., et al. 2008, *A&A*, 486, 951
- [13] Heiter, U., Lind, K., Bergemann, M., et al. 2021, *A&A*, 645, A106
- [14] Hunt, E. L., & Reffert, S. 2023, *A&A*, 673, A114
- [15] Jofré, P., Heiter, U., Soubiran, C., et al. 2015, *A&A*, 582, A81
- [16] Lagarde, N., Decressin, T., Charbonnel, C., et al. 2012, *A&A*, 543, A108
- [17] Nguyen, C. T., Costa, G., Girardi, L., et al. 2022, *A&A*, 665, A126
- [18] Önehag, A., Korn, A., Gustafsson, B., Stempels, E., & Vandenberg, D. A. 2011, *A&A*, 528, A85
- [19] Spina, L., Magrini, L., & Cunha, K. 2022, *Universe*, 8, 87